Epitaxial growth and magnetic properties of Fe_3O_4 films on TiN buffered Si(001), Si(110), and Si(111) substrates

Hua Xiang,[1,a)] Fengyuan Shi,[1] Mark S. Rzchowski,[2] Paul M. Voyles,[1] and Y. Austin Chang[1,a)]
[1]*Department of Materials Science and Engineering, University of Wisconsin-Madison, Madison, Wisconsin 53706, USA*
[2]*Department of Physics, University of Wisconsin-Madison, Madison, Wisconsin 53706, USA*

(Received 25 May 2010; accepted 7 August 2010; published online 2 September 2010)

Epitaxial Fe_3O_4 thin films were grown on TiN buffered Si(001), Si(110), and Si(111) substrates by dc reactive sputtering deposition. Both Fe_3O_4 films and TiN buffer are fully epitaxial when grown at substrate temperatures above 150 °C, with textured single phase Fe_3O_4 resulting from room temperature growth. The initial sputtered Fe_3O_4 formed nuclei islands and then coalesced to epitaxial columnar grains with increasing film thickness. The magnetization decreases and the coercive field increases with decreasing film thickness. There is no in-plane magnetic anisotropy of epitaxial Fe_3O_4(001) on Si(001) but Fe_3O_4 films grown on Si(110) and Si(111) substrates show uniaxial in-plane magnetic anisotropy. © *2010 American Institute of Physics*.
[doi:10.1063/1.3484278]

Theoretical calculations predict that Fe_3O_4 exhibits not only half metallic properties at room temperature (RT) but also a negative spin polarization (SP). Combined with the high Curie temperature of ~860 K, Fe_3O_4 is one of the most promising magnetic materials for spintronic devices.[1–3] Because of the near-perfect lattice match between Fe_3O_4 and MgO, epitaxial Fe_3O_4 films have been mainly grown on MgO substrates.[4,5] However, for the purpose of developing the next generation of spintronic devices, epitaxial growth of high quality Fe_3O_4 films on semiconductors, particularly Si, is of great technological importance.[6,7]

The crystalline structures of Fe_3O_4 films directly deposited on Si show varying results, from amorphous to polycrystalline, with some reports of oriented growth.[2,8–11] Although (111) texture of Fe_3O_4 on Si has been reported,[10,11] the films have undesirable and complex Fe_3O_4/Si interfaces. Examples are magnetic iron silicide, amorphous oxide, and weakly coupled phases of FeO and Fe_2O_3; all of which adversely affect the properties of the resulting Fe_3O_4 films.[9,11] Given the relatively large lattice mismatch between Fe_3O_4 and Si, a buffer layer is likely needed to induce the Fe_3O_4 epitaxial growth on Si. Investigations of Fe_3O_4 films deposited on Si with buffer layers of Ti, Ta, SiO_2, and Fe_2O_3 all show results of polycrystalline Fe_3O_4.[12,13] Hassan *et al.*[6] grew epitaxial Fe_3O_4 on Si(001) using an MgO buffer. However, it is reported that the MgO/Fe_3O_4 bilayer suffers interdiffusion at relatively low temperatures, starting from about 250–300 °C and becoming severe above ~430 °C.[14] Reisinger *et al.*[15] fabricated and characterized epitaxial Fe_3O_4 on Si(001) using TiN/MgO buffer but did not report the magnetic properties. In this paper, we report the preparation of Fe_3O_4(001), Fe_3O_4(110), and Fe_3O_4(111) epitaxial films on TiN buffered Si by reactive sputtering. The effects of the substrate temperature, sputtering power, film thickness, and Si substrate orientations on the crystalline and magnetic properties of Fe_3O_4 films were investigated; and the uniaxial in-plane magnetic anisotropies of epitaxial Fe_3O_4(110) and Fe_3O_4(111) films were reported.

Multilayer stacks with the structure of substrate/TiN(10)/Fe_3O_4(t) (nanometer) were grown by dc magnetron reactive sputtering in a home-built system with base pressure better than 1.0×10^{-7} Torr. Si wafers with orientations of (001), (110) and (111) were used as the substrates. The TiN buffer was prepared at 550 °C.[16] After the substrate was cooled to RT, the Fe_3O_4 layer with different thickness (t) was deposited on the TiN/Si structure at substrate temperatures (T_s) of RT, 150, 250, 300, and 400 °C, by three different dc sputtering powers, 30, 60, and 120 W.

Figures 1(a)–1(c) show the θ-2θ scans of the 270 nm Fe_3O_4 films grown on TiN buffered substrates of Si(001), Si(110), and Si(111) at T_s=300 °C respectively. Since the lattice parameter of Fe_3O_4 (a=0.8396 nm) is almost exactly twice that of TiN (a=0.4242 nm), the main peaks of these two films are very close to each other, and Fig. 1(a) shows an overlap peak of TiN(200) and Fe_3O_4(400) near 43.2° along with a Si(400) peak. The Φ scan patterns of the Fe_3O_4(311) and Si(311) pole at azimuth angle of 25.24° [inset to Fig. 1(a)] show fourfold symmetry and indicate the epitaxial growth of the Fe_3O_4 on TiN buffered Si(001). Since our previous studies[16] showed TiN can grow epitaxially on Si(001), we conclude that the crystallographic relationship of the entire stack is Si(004)[100]‖TiN(002)[100]‖Fe_3O_4(004)[100]. For Fe_3O_4 deposited on TiN buffered Si(111), the θ-2θ scan shows peaks corresponding to Fe_3O_4{111} family and Si(111), as shown in Fig. 1(b). The inset to Fig. 1(b) shows the epitaxial crystallographic relationship can be determined as Si(111)[100]‖TiN(111)[100]‖Fe_3O_4(111)[100]. The case of the epitaxial Fe_3O_4 film on Si(110) substrate shows in Fig. 1(c), and the crystallographic relationship of the entire stack is Si(220)[100]‖TiN(220)[100]‖Fe_3O_4(440)[100].

The substrate temperature plays an important role in determining the epitaxial film quality. For the Fe_3O_4 film grown on TiN buffered Si(001) at RT, x-ray diffraction (XRD) results show that the film is a mixture of (400) pre-

a)Electronic mail: xiang2@wisc.edu and changy@cae.wisc.edu.

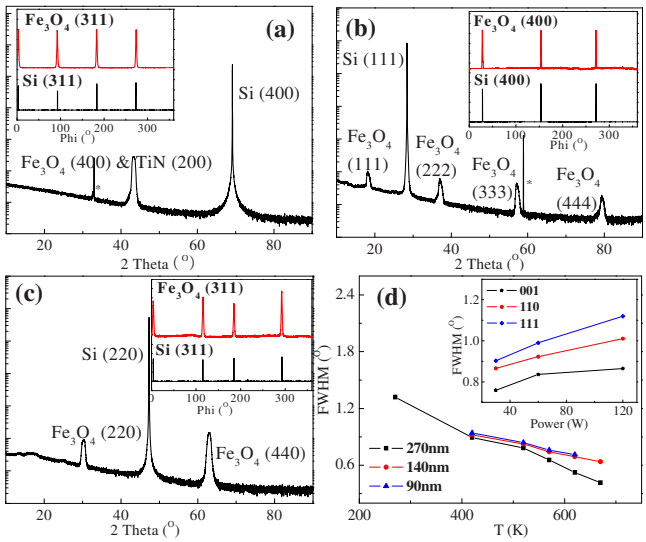

FIG. 1. (Color online) The θ-2θ scan of 270 nm Fe_3O_4 films on TiN buffered (a) Si(001), (b) Si(111), and (c) Si(110) substrates; and also (d) the rocking curve FWHM data of the Fe_3O_4 films prepared at different T_s and by different sputtering powers. (Peak lines indicated by ∗ are from the substrates.)

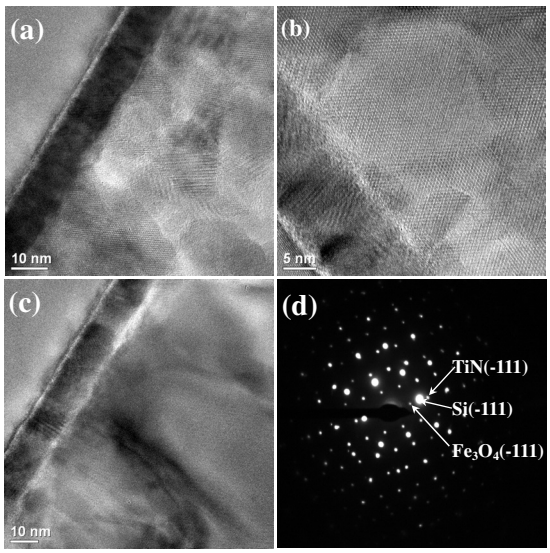

FIG. 2. Low magnification and HR-TEM images along the Si(110) zone axis of the 270 nm Fe_3O_4 films deposited on TiN buffered Si(001) at (a) RT, and (b) and (c) 250 °C; (d) selective area diffraction pattern of the entire Si(001)/TiN/Fe_3O_4 stack.

ferred texture with some (440) oriented structures (results not shown here). After increasing the T_s to 150 °C, the epitaxial quality of the resulting Fe_3O_4 film improved drastically with no misoriented structures detected with XRD. Figure 1(d) shows the rocking curve full width at half maximum (FWHM) data of Fe_3O_4(400) peak of 90, 140, and 270 nm Fe_3O_4 films on Si(001) at different T_s, respectively. The data decrease rapidly with increasing T_s, indicating a decreasing mosaic spread. The rocking curve width also decreases with increasing film thickness, i.e., thicker films show better epitaxial quality, and this should be related to the sputtered Fe_3O_4 film growth mechanism which will be explained in later parts. The inset of Fig. 1(d) shows the FWHM data of 90 nm Fe_3O_4 films on the three Si substrates prepared using 30, 60, and 120 W dc powers at T_s=400 °C, and the Fe_3O_4 films grown at lower sputtering powers show narrower rocking curves. Typically, the sputtering rate decreases with lower powers if the power is the only variable, and slow sputtering rates may be helpful to improve the Fe_3O_4 film epitaxial quality.[4]

Figure 2 shows the low magnification and high resolution transmission electron microscopy (HR-TEM) images of the epitaxial Fe_3O_4 film on Si(001) at T_s=RT and 250 °C, respectively. From Fig. 2(a), combined with the XRD results, the Fe_3O_4 film prepared at RT is a mixture of mainly (400) texture and some polycrystalline domains. Figs. 2(b) and 2(c) show the images of Si/TiN/Fe_3O_4 stack at T_s=250 °C along the Si(110) zone axis. With the elevated T_s, the Fe_3O_4 film becomes more condensed and the grain size also increases. The different contrast of these two images is due to the intrinsic antiphase boundaries (APBs). APBs have been well documented in epitaxial Fe_3O_4/MgO systems,[4,5] and they are also present in our Fe_3O_4/TiN structures given the very close lattice parameters between TiN and MgO. Combined Figs. 2(a) and 2(c) we find an initial layer of about 10–20 nm Fe_3O_4 film grows as island nuclei and then coalesces to epitaxial columnar larger grains with the increasing film thickness.[2] The 10 nm TiN buffers are very smooth on all three Si substrates, with the atomic force microscopy measured rms=0.21±0.03 nm on Si(001), 0.23±0.03 nm on Si(110) and 0.18±0.03 nm on Si(111). However, the scanning transmission electron microscopy energy dispersive spectroscopy measurements show there is a ~2 nm intermixing layer at the TiN/Fe_3O_4 interface, with 8.21±0.56 at. % Ti diffusion into Fe_3O_4, which may affect the magnetic property. The electron diffraction pattern of the whole stack in Fig. 2(d) confirms the overall epitaxial relationship between Si, TiN, and Fe_3O_4 is quite good.

Figure 3(a) shows the high resolution x-ray photoemission spectroscopy (XPS) spectra of the Fe 2*p* region of Fe_3O_4 films at T_s=150 and 400 °C. The broad Fe 2*p* peaks, attributed to the coexistence of Fe^{3+} and Fe^{2+} states, exclude the possible presence of Fe_2O_3.[17] Fig. 3(b) shows the RT magnetization hysteresis loops of the 270 nm Fe_3O_4 films at different T_s on Si(001). The effects of the Si/TiN bilayer have been subtracted in this study. The magnetization (M) of the Fe_3O_4 film is not completely saturated up to 6000 Oe. This is a well documented behavior of epitaxial Fe_3O_4 films,[12,18] attributed to the intrinsic APBs arising from iron sublattice stacking faults. These stacking faults result in strong antiferromagnetic (AF) exchange coupling between adjacent antiphase domains.[18,19] It is difficult to overcome this coupling and magnetically align adjacent domains even in moderate magnetic field. The T_s has evident effects on

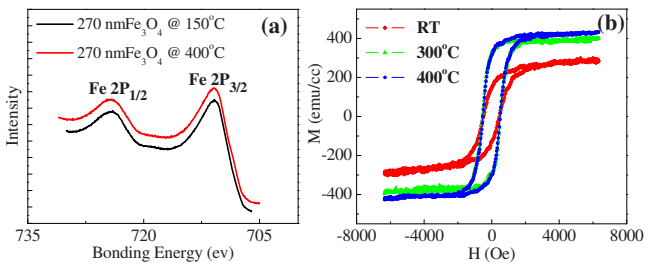

FIG. 3. (Color online) (a) The high resolution XPS spectra of the Fe 2*p* region of Fe_3O_4 films at T_s=150 and 400 °C; (b) the RT magnetization hysteresis loops of 270 nm Fe_3O_4 films prepared at different T_s on TiN buffered Si(001).

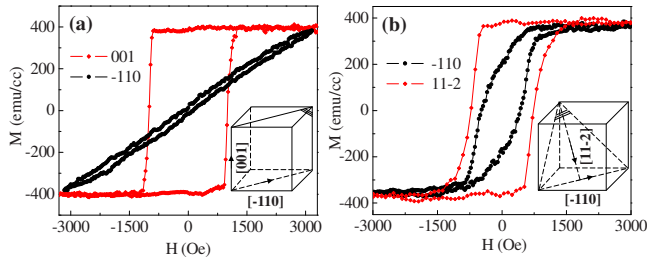

FIG. 4. (Color online) The RT magnetization loops of 90 nm Fe_3O_4 films grown at T_s=300 °C on (a) Si(110) and (b) Si(111) substrate.

the magnetization improvement of the films, from 290 ± 20 emu/cc at RT to 420 ± 20 emu/cc at T_s=400 °C of our 270 nm Fe_3O_4 films, primarily resulting from a larger domain size and lower APB density with elevated T_s. The coercive fields (Hc) are approximately independent of growth temperature, 490 ± 20 Oe for 270 nm films.

We investigated the thickness dependence of the magnetic properties by comparing the 270, 140, and 90 nm Fe_3O_4 films grown on Si(001) at T_s=400 °C. The M decreases from 420 ± 20, 380 ± 20, to 310 ± 20 emu/cc, and the Hc increases from 490 ± 20, 530 ± 20, to 570 ± 20 Oe for these thicknesses. The main reason for such a variation in M and Hc is likely the shrinking antiphase domain sizes and the increasing effects of APBs with smaller t. Eerenstein *et al.*[20] has reported a $t^{-1/2}$ power relationship between the Fe_3O_4 film thickness t and the APBs density. More APBs mean more AF couplings, intuitively resulting in smaller M. A second reason is based on the film growth mechanism of initial island nuclei coalescence followed by columnar grain growth. The out-of-plane orientations of the Fe_3O_4 grains in the initial layer might scatter to a certain extent. However, with increasing thickness, the subsequent epitaxial columnar Fe_3O_4 grains grow, resulting in relatively lower Hc due to fewer defects. The third reason could be the relatively larger epitaxial strain in thinner films, which may cause strain-induced magnetic property variations.[1,6,7,10]

We also studied the in-plane magnetic anisotropy of the Fe_3O_4 films on the three Si substrates. There is no magnetic anisotropy between {100} and {110} directions of the films grown on Si(001) substrates. However, both epitaxial Fe_3O_4 films on Si(110) and Si(111) substrates show uniaxial in-plane magnetic anisotropy at RT, as shown in Figures 4(a) and 4(b). For the Fe_3O_4 film on Si(110), the [001] direction is the in-plane easy axis in Fig. 4(a). This is in contradiction to the previously reported results of epitaxial Fe_3O_4 films on MgO(110) substrate, which have $[\bar{1}10]$ in-plane easy axis.[1,4] By assuming an isotropic 0.3% strain for epitaxial Fe_3O_4 on MgO(110), Aoshima and Wang[1] calculated the magnetoelastic and magnetocrystalline energy of $[\bar{1}10]$ and [001] directions respectively, and found the relatively larger difference of the magnetoelastic energies between these two directions leads to a strain-induced $[\bar{1}10]$ easy axis. However, the lattice mismatch between Fe_3O_4 and TiN (about 1.1%) is much larger than that between Fe_3O_4 and MgO, and may cause the difference. Moreover, the M and Hc along the [001] direction are 385 ± 20 emu/cc and 1000 ± 20 Oe, respectively. Fig. 4(b) shows the in-plane magnetic anisotropy of Fe_3O_4(111) film on Si(111), with the easy axis determined as $[11\bar{2}]$. The corresponding M and Hc along $[11\bar{2}]$ are 375 ± 20 emu/cc and 730 ± 20 Oe, respectively.

In conclusion, the sputtered epitaxial Fe_3O_4 films on Si substrates and the corresponding magnetic properties were reported. Both Fe_3O_4 films grown on Si(110) and (111) substrates show uniaxial in-plane magnetic anisotropy and the easy axes are determined as [001] and $[11\bar{2}]$, respectively. The [001] easy axis of the epitaxial Fe_3O_4(110) film on TiN/Si(110) is opposite to the reported results of Fe_3O_4/MgO(110), which may relate to the relatively larger lattice mismatch between Fe_3O_4 and TiN. The magnetization of (110)- and (111)-oriented Fe_3O_4 films are comparable but the coercive field of Fe_3O_4(111) film is much smaller than that of Fe_3O_4(110) film. For epitaxial Fe_3O_4 films on the three Si substrates, both the in-plane and out-of-plane crystallographic directions of Fe_3O_4, TiN, and the corresponding Si substrates are parallel to one another. The epitaxial growth of Fe_3O_4 on Si and the reported magnetic properties should be helpful to engineer the magnetic tunnel junctions with Fe_3O_4 electrodes or other spintronic devices.

This work is supported by the Office of Basic Energy Research of DOE through Grant No. DE-FG02-99-ER45777, the Wisconsin Alumni Research Foundation (WARF), and the Wisconsin Distinguished Professorship.

[1]K.-I. Aoshima and S. X. Wang, J. Appl. Phys. **91**, 7146 (2002).
[2]Y. Peng, C. Park, and D. E. Laughlin, J. Appl. Phys. **93**, 7957 (2003).
[3]Z. Zhang and S. Satpatahy, Phys. Rev. B **44**, 13319 (1991).
[4]D. T. Margulies, F. T. Parker, M. L. Rudee, F. E. Spada, J. N. Chapman, P. R. Aitchison, and A. E. Berkowitz, Phys. Rev. Lett. **79**, 5162 (1997).
[5]J. M. D. Coey, A. E. Berkowitz, L. I. Balcells, F. F. Putris, and F. T. Parker, Appl. Phys. Lett. **72**, 734 (1998).
[6]S. S. A. Hassan, Y. Xu, J. Wu, and S. M. Thompson, IEEE Trans. Magn. **45**, 4357 (2009).
[7]P. K. J. Wong, W. Zhang, X. G. Cui, Y. B. Xu, J. Wu, Z. K. Tao, X. Li, Z. L. Xie, R. Zhang, and G. van der Laan, Phys. Rev. B **81**, 035419 (2010).
[8]J. Tang, K.-Y. Wang, and W. Zhou, J. Appl. Phys. **89**, 7690 (2001).
[9]S. Jain, A. O. Adeyeye, and D. Y. Dai, J. Appl. Phys. **95**, 7237 (2004).
[10]R. J. Kennedy and P. A. Stampe, J. Phys. D: Appl. Phys. **32**, 16 (1999).
[11]C. Boothman, A. M. Sánchez, and S. V. Dijken, J. Appl. Phys. **101**, 123903 (2007).
[12]S. Jain, A. O. Adeyeye, and C. B. Boothroyd, J. Appl. Phys. **97**, 093713 (2005).
[13]D. Tripathy, A. O. Adeyeye, and C. B. Boothroyd, J. Appl. Phys. **99**, 08J105 (2006).
[14]K. A. Shaw, E. Lochner, and D. M. Lind, J. Appl. Phys. **87**, 1727 (2000).
[15]D. Reisinger, M. Schonecke, T. Brenninger, M. Opel, A. Erb, L. Alff, and R. Gross, J. Appl. Phys. **94**, 1857 (2003).
[16]H. Xiang, C.-X. Ji, J. J. Yang, and Y. A. Chang, Appl. Phys. A: Mater. Sci. Process. **98**, 707 (2010).
[17]A. Fujimori, M. Saeki, N. Kimizuka, M. Taniguchi, and S. Suga, Phys. Rev. B **34**, 7318 (1986).
[18]D. T. Margulies, F. T. Parker, F. E. Spada, R. S. Goldman, J. Li, R. Sinclair, and A. E. Berkowitz, Phys. Rev. B **53**, 9175 (1996).
[19]P. Li, L. T. Zhang, W. B. Mi, E. Y. Jiang, and H. L. Bai, J. Appl. Phys. **106**, 033908 (2009).
[20]W. Eerenstein, T. Palstra, T. Hibma, and S. Celotto, Phys. Rev. B **68**, 014428 (2003).